Solitary Vortex Pairs in Viscoelastic Couette Flow

Alexander Groisman and Victor Steinberg

Department of Physics of Complex Systems, The Weizmann Institute of Science, 76100 Rehovot, Israel
(Received 8 November 1996)

We report experimental observation of a localized structure, which is of a new type for dissipative systems. It appears as a solitary vortex pair ("diwhirl") in Couette flow with highly elastic polymer solutions. In contrast to the usual solitons the diwhirls are *stationary*. It is also a new object in fluid dynamics—a pair of vortices that build a single entity. The diwhirls arise as a result of a purely elastic instability through a hysteretic transition at negligible Reynolds numbers. It is suggested that the vortex flow is driven by the same forces that cause the Weissenberg effect. [S0031-9007(97)02429-0]

PACS numbers: 47.54.+r, 47.50.+d, 61.25.Hq, 83.50.Eb

Stable spatially localized structures have been observed in many conservative and weakly dissipative systems [1,2]. They have a form of waves with a spatially modulated amplitude. These solitary waves are stabilized by a balance between the wave dispersion and nonlinearity. In weakly dissipative systems they usually arise as a result of a hysteretic transition, while the dissipation is selecting a unique amplitude profile and group velocity [3]. Quite recently, oscillatory solitary structures have been found in strongly dissipative parametrically driven systems [4,5]. We report here the observation of a new type of localized structure which is *stationary* and appears as a pair of vortices in rotating Couette flow. These solitary vortex pairs arise as a result of a purely elastic instability (at very low Reynolds numbers), if the working fluid is a highly elastic polymer solution. Like in Refs. [4,5], the system is highly dissipative and the transition is strongly hysteretic.

A Couette-Taylor (CT) column is a simple arrangement of two coaxial cylinders with a working fluid in the annular gap between them. If the fluid is Newtonian, the outer cylinder is stationary, and the inner cylinder is rotating, at some rotation velocity Ω_T a pattern of toroidal vortices appears on the background of the basic purely azimuthal flow (Couette flow) [6]. These Taylor vortices are stationary and build an axially periodic axisymmetric array. They arise because the balance between the centrifugal force experienced by the rotating fluid and the radial pressure gradient is unstable with respect to radial motion of the fluid. This instability is locally symmetric with respect to the fluid motion outwards (outflow) and inwards (inflow), so inflow and outflow in the Taylor vortices look rather similar.

The behavior of viscoelastic liquids in the CT geometry can be quite different from that of the usual Newtonian fluids. If, for example, a vertical rotating rod is inserted in a beaker with a highly elastic polymer solution, the liquid starts to climb up on it, instead of being pushed outward by the centrifugal force. The reason for this "rod climbing" (Weissenberg effect) [7,8] is that the rod rotation produces a shear flow, which stretches the polymer molecules around the rod in the azimuthal direction. These elongated molecules act as stretched rubber rings that push the liquid towards the rod ("hoop stress"). In other words, one can say that stretching of the polymer molecules along the streamlines leads to a negative normal stress difference $N_1 = \sigma_{\theta\theta} - \sigma_{rr}$, where r, θ, and z are cylindrical coordinates. Since the cylindrical geometry is curvilinear, this negative N_1 produces a volume force acting inwards in the radial direction that causes the rod climbing.

Therefore, it is natural to suppose that for a highly elastic polymer solution the character of instability in the Couette flow will be different as well. In particular, shear rate and solution elasticity, instead of the fluid velocity and density, should now come into play. A possible instability mechanism was proposed by Larson, Shaqfeh, and Muller [9]. To describe the polymer solution rheology, they used the elastic dumbbell model [7], where a polymer molecule is modeled by two beads connected by a spring. For the Couette flow it gives $N_1 \sim \langle R_r^2 \rangle (\tau \dot{\gamma}_{r\theta})^2$. Here $\langle R_r^2 \rangle$ is the average square of the r component of the vector $\vec{R}$ connecting the beads of a dumbbell, $\dot{\gamma}_{r\theta}$ is shear rate, and τ is the polymer relaxation time. $\langle R_r^2 \rangle$ is proportional to the temperature of the liquid and is not affected by the Couette flow. The nondimensional combination $\tau \dot{\gamma}_{r\theta}$ is called the Deborah number De, so the azimuthal stretching of the dumbbells and the hoop stress are proportional to $\langle R_r^2 \rangle$ and De^2. Any radial fluid motion in the CT column implies regions with positive $\partial v_r / \partial r$ that corresponds to an elongational flow. Such a flow stretches the dumbbells in the radial direction and increases $\langle R_r^2 \rangle$. This radial stretching is coupled to the strong primary shear flow and causes additional azimuthal elongation and growth of N_1 and the hoop stress. This increased hoop stress reacts back on the flow driving the radial motion.

An important feature of this mechanism that was not discussed in Ref. [9] is its asymmetry with respect to the radial motion outwards and inwards. A fluid particle that starts its radial motion in any direction should be first accelerated. This implies positive $\partial v_r / \partial r$, radial stretching of the dumbbells, and local growth of N_1 and hoop stress. This increased local hoop stress will

accelerate a fluid particle moving inwards and slow down the outward motion. Therefore, one can expect the vortex patterns to have major differences between the inflow and the outflow.

We conducted our experiments in a temperature-controlled CT column with the inner cylinder radius $R_1 = 34$ mm, the gap $d = 7$ mm, and the length $L = 516$ mm. As an elastic liquid, we used a 300 ppm solution of high molecular weight PAAm [10] in a viscous Newtonian solvent which was a 63% solution of saccharose in water. Solution viscosity and relaxation time were measured with the aid of a commercial viscometer [10]. In the explored temperature region of $5-37.5\,°C$ the ratio of the solution viscosity to the solvent viscosity was practically constant at $\eta/\eta_s = 1.82$, while η_s changed from 0.35 to 2.9 P. The polymer relaxation time τ approximately followed $\tau \sim \eta_s/T^3$ (T is the absolute temperature). Thus, by changing the temperature in the CT column from 37.5 to 5 °C we could change τ from 0.28 to 3.1 s.

The flow in the CT column was visualized by three different methods. Adding to the working liquid a moderate amount of light reflecting flakes (0.6% of the Kalliroscope liquid) we observed the flow in the ambient illumination. In order to visualize the flow profile across the gap in r-z cross section, we used the light sheet technique. A small amount of the light reflecting flakes (0.1% of Kalliroscope) was added to the working liquid and a laser beam expanded by a cylindrical lens to a sheet of light parallel to the column axis was used for illumination. We also directly measured axial and radial components of the fluid velocity with the aid of a laser Doppler velocimeter (LDV).

The sequence of flow patterns in the CT column was the same in the whole studied region of τ (Fig. 1). As the rotation velocity was raised, at some critical value Ω_0 the basic Couette flow became unstable and a pattern of chaotically oscillating vortices appeared in the column [Fig. 1(a)]. This pattern ("disordered oscillations") was described in Ref. [10]. The transition was abrupt and
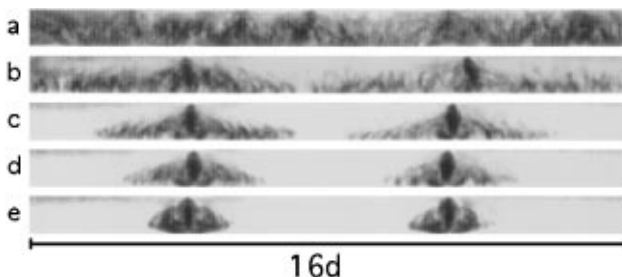
strongly hysteretic. If Ω was lowered afterwards, first the vortex motion became concentrated close to the inner cylinder except for the regions near black spindle-shaped cores [Fig. 1(b)]. Then, at a lower velocity, the pattern became spatially inhomogeneous [Fig. 1(c)]. The oscillating vortices were localized inside separate strips with a core in the middle. As the rotation velocity was decreased further, these oscillatory strips became narrower [Fig. 1(d)] until at some Ω the oscillations ceased and stationary vortex structures appeared [Fig. 1(e)]. The stationary structures decayed and the Couette flow finally recovered at a rotation velocity Ω_c that could be as low as $0.45\Omega_0$. These stationary localized structures shown in Fig. 1(e), which we call solitary vortex pairs or "diwhirls," are the subject of this Letter.

A typical pattern of diwhirls in the CT column is shown in Fig. 2. The diwhirls appear as randomly spaced axisymmetric dark rings. The dark color here, just as the dark color of the spindle-shaped cores of the diwhirls in Fig. 1(e), indicates regions of intensive radial flow. Figure 3 presents a typical dependence of the radial velocity v_r on the axial position. A typical distribution of the axial velocity v_z along the cylinder axis in an isolated diwhirl is shown in Fig. 4. v_z exponentially decreases toward the diwhirl edges with a characteristic length of about $0.7d$. Figure 5 shows a schematic drawing of the flow lines of a diwhirl in the rz plane, as it follows from Figs. 1(e), 3, and 4. They somewhat resemble the field lines of a magnetic dipole. One can see that every diwhirl is really a pair of vortices having a common core—a narrow region, about $0.5d$ in width, of fast fluid motion *inwards*. The outflow is slow and spreads over regions of about $2.5d$ at both sides of the core, decaying at the vortex edges. The diwhirls are, thus, localized within strips of about $5d$ along the column axis, the flow between them being just the unperturbed Couette flow. The velocity profiles of different diwhirls are strikingly similar (Fig. 3). They are symmetric (which implies that the vortices in the diwhirls are just mirror images of each other), have the same width and height, and even the same peculiarities in the outward velocity—local minima at about $0.75d$ from the center. This form of the diwhirl velocity profile was also independent of τ.

The axial position of an isolated diwhirl can be quite stationary, changing by less than 0.1 mm per hour. If,

FIG. 1. Various flow patterns that are observed as Ω decreases from Ω_0 to Ω_c. The flow was visualized with the aid of the light sheet technique. The top and the bottom of each strip correspond to the outer and the inner cylinders, respectively. (a) $\Omega = \Omega_0$; (b) $\Omega = 0.75\Omega_0$; (c) $\Omega = 0.69\Omega_0$; (d) $\Omega = 0.59\Omega_0$; (e) $\Omega = 0.48\Omega_0$. $\Omega_c = 0.47\Omega_0$.
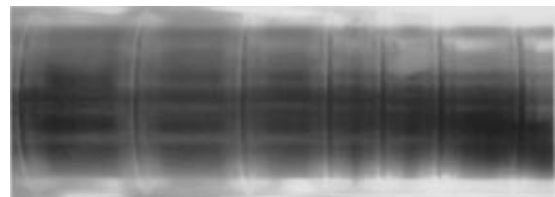

FIG. 2. A photograph of the CT column with a diwhirl pattern. A similar pattern was reported in a different polymer solution [12].
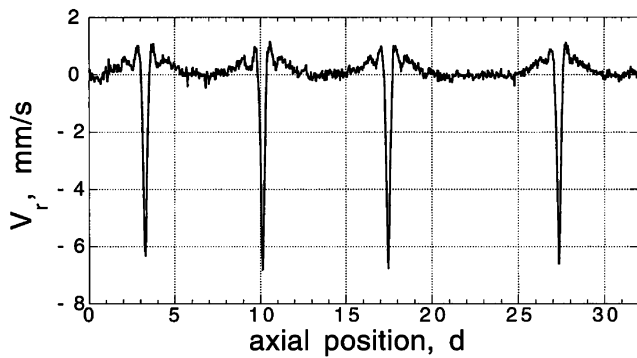
FIG. 3. Radial component of the fluid velocity v_r, measured by LDV at a constant radius (near the middle of the gap, where v_r is maximal), as a function of position along the column axis.

however, the distance between two diwhirls is less than about $5d$, they move towards each other and finally coalesce (Fig. 6). It is quite noticeable that the "daughter" diwhirl has the same shape as both its "parents," which is another manifestation of the universality of the diwhirl profiles. One can also see that the daughter diwhirl inherited the two vortices that used to be at the outer sides of the parent diwhirls, while those two which used to be at their inner sides just annihilated. The energy of the vortices that disappear is first transferred to a wavy motion [Fig. 6(d)] and then dissipates [Fig. 6(e)]. Dependence of the distance between the diwhirl centers on time was identical for different merging events, which occurred at a particular τ and Ω. It is shown in Fig. 7, where the distance is plotted as a function of time for five distinct mergings. Quite naturally, the diwhirl interaction becomes stronger as they get closer.

The final diwhirl separation depends on the flow history. If the rotation velocity is quenched from above Ω_0 to slightly above Ω_c, at first a lot of closely spaced diwhirls are produced. The diwhirls then start to move towards each other and merge. This merging continues
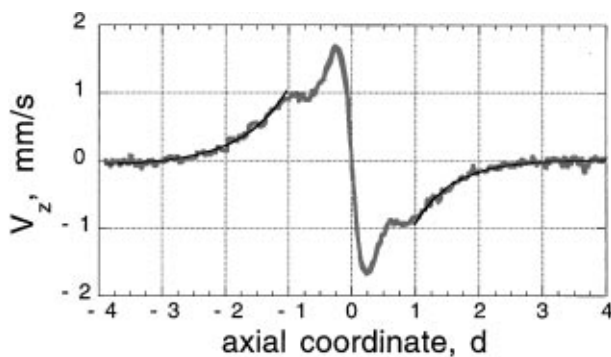

FIG. 4. Axial component of the fluid velocity in a diwhirl v_z as a function of axial position (thick grey curve). v_z was measured by LDV at a constant radius near the inner cylinder, where it is maximal. The velocity at the diwhirl edges is fitted by exponents $1.36/d$ and $-1.64/d$ (thin black lines).
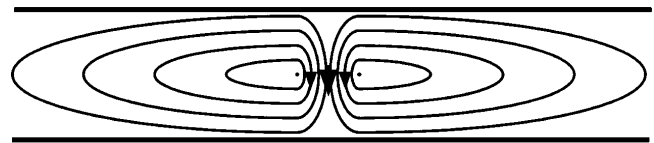

FIG. 5. Schematic drawing of the flow lines in a diwhirl.

until the distance between neighboring diwhirls reaches the "safe" value of about $5d$. In general, the number of diwhirls at fixed Ω varied from one to about a dozen depending on the flow history.

Strong evidence for the elastic origin of the diwhirls is that, in the explored region of τ, the Deborah number at Ω_c, $De_c = \Omega_c\tau R_1/d$, remained constant (up to 5%) at about 10. It means that the diwhirls always decayed at the same value of the hoop stresses. In the same region of τ, the Reynolds number at Ω_c decreased from 33% to 0.4% of its critical value corresponding to Ω_T, making the inertial instability mechanism completely irrelevant. Further, the maximal radial velocity in diwhirls was found to be inversely proportional to the elastic relaxation time, so that $v_{r,\max} \simeq 0.5d/\tau$ at Ω_c.

The major asymmetry between the inflow and outflow in diwhirls (Fig. 3) was conceived above from the general properties of the elastic instability mechanism. The forces driving the diwhirl flow can be understood in more details from the following arguments. Although in the laboratory frame the flow in a diwhirl appears as stationary, in the reference frame of moving fluid (Lagrangian coordinates) the rate of strain changes periodically as a fluid particle moves along the flow lines (Fig. 5). Since conformation of a polymer molecule depends on the history of deformations of the fluid element inside which the molecule resides, it is the Lagrangian coordinates that should be used for estimation of the elastic stresses. When a fluid particle starts its radial motion, it is in a region of positive $\partial v_r/\partial r$ in both inflow and outflow (Fig. 5). v_r becomes maximal near the middle of the gap, and after crossing the point of maximal v_r the fluid particle enters the region of negative $\partial v_r/\partial r$ and contractional flow. The
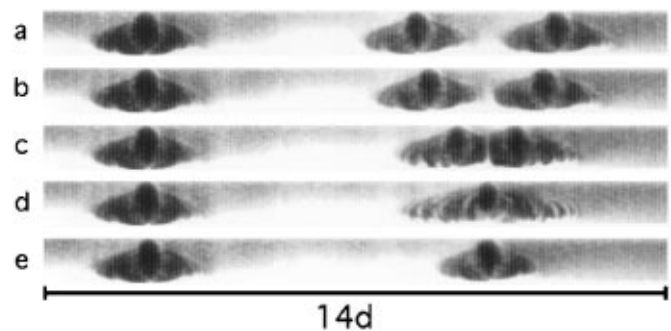

FIG. 6. The consecutive stages of coalescence of two closely spaced diwhirls (the visualization technique was the same as in Fig. 1).
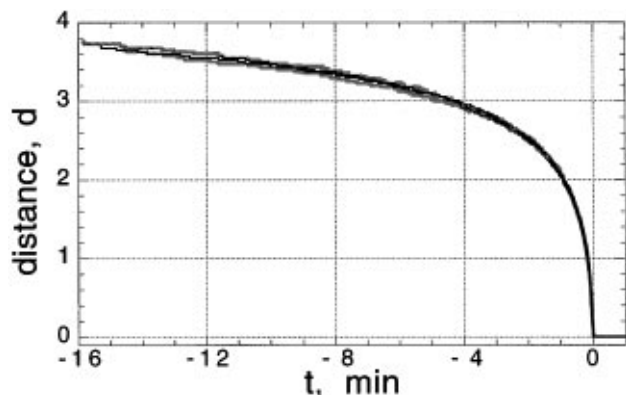
FIG. 7. Distance between the diwhirl centers as a function of time for five separate merging events (gray and black curves). The initial distances were different; the moment of coalescence was taken as $t = 0$.

characteristic time of these variations in $\partial v_r / \partial r$ experienced by the particle is just d/v_r, where v_r is a typical radial velocity. In the diwhirl outflow the radial motion is slow, so that $d/v_r \gg \tau$ and the radial elongation of the polymers always corresponds to the current $\partial v_r / \partial r$. It implies that the average elongation across the gap is zero, since the regions of elongational flow (positive $\partial v_r / \partial r$) are exactly compensated by the contractional flow regions. Therefore, the additional hoop stresses produced by the outflow are averaged to zero, when integrated across the gap, and have small influence on this slow flow. If, however, the radial flow is fast enough, so that $d/v_r \simeq \tau$, like in the diwhirl inflow, there exists a significant phase lag between $\partial v_r / \partial r$ and the radial polymer elongation. Then $\langle R_r^2 \rangle$ depends not only on $\partial v_r / \partial r$ but also on its time integral. The latter is always positive, since the elongation always comes before the contraction as a fluid particle moves along the radius. Thus, the additional hoop stress averaged across the gap is positive in this case, which results in a radial force that acts in the inward direction and drives the inflow.

The narrow diwhirl core turns out to be the region where the energy is pumped into the diwhirls. In the Lagrangian coordinates v_r/d plays a role of frequency, which should be large enough to assure a nonzero average radial elongation. That is why diwhirls arise as a result of a hysteretic transition and have finite v_r before their decay at Ω_c. Analyzing statistical distributions of v_r in the chaotic oscillatory flows shown in Figs. 1(a)–1(d), we found that the major asymmetry between the inflow and the outflow is present there as well. Therefore, we believe that this asymmetry is a general feature of the flow instabilities driven by the hoop stress and the proposed instability mechanism has wide applicability.

Pattern formation in many dissipative systems has been successfully described by the amplitude equation [1]. This equation, however, does not have stationary localized solutions and, thus, cannot be adequate for the diwhirls. Nevertheless, such solutions can exist if the amplitude equation describes a hysteretic transition and is coupled to another dynamic equation for a slow mode [11]. In our case, this slow mode could represent the elastic stresses which drive the fluid motion.

[1] M. C. Cross and P. C. Hohenberg, Rev. Mod. Phys. **65**, 851 (1993).
[2] A. C. Newell, *Solitons in Mathematics and Physics* (Society for Industrial and Applied Mathematics, Philadelphia, 1985).
[3] S. Fauve and O. Thual, Phys. Rev. Lett. **64**, 282 (1990).
[4] O. Lioubashevski, H. Arbel, and J. Fineberg, Phys. Rev. Lett. **76**, 3959 (1996).
[5] P. B. Umbanhowar, F. Melo, and H. L. Swinney, Nature (London) **382**, 793 (1996).
[6] G. I. Taylor, Philos. Trans. R. Soc. London A **223**, 289 (1923).
[7] R. B. Bird, Ch. Curtiss, R. C. Armstrong, and O. Hassager, *Dynamics of Polymeric Liquids* (Wiley, New York, 1987), Vols. 1 and 2.
[8] K. Weissenberg, Nature (London) **159**, 310 (1947).
[9] R. G. Larson, E. S. G. Shaqfeh, and S. J. Muller, J. Fluid Mech. **218**, 573 (1990).
[10] A. Groisman and V. Steinberg, Phys. Rev. Lett. **77**, 1480 (1996).
[11] H. Riecke, Physica (Amsterdam) **92D**, 69 (1995).
[12] R. Haas and K. Bühler, Rheol. Acta **28**, 402 (1989).